STOCHASTIC FINITE FAULT MODELING FOR THE 16 SEPTEMBER 1978 TABAS, IRAN, EARTHQUAKE

S. Yaghmaei-Sabegh

Department of Civil Engineering, University of Tabriz
P.O Box 51666-16471 Tabriz, Iran, s_yaghmaei@tabrizu.ac.ir

(Received: November 9, 2008 – Accepted in Revised Form: March 11, 2010)

Abstract The main objective of this study is estimating acceleration time history of 16 September 1978 Tabas earthquake incorporating the seismological/geological source-path and site model parameters by using finite-fault simulation approach. The method generalizes the stochastic ground-motion simulation technique, developed for point sources, to the case of finite faults. It subdivides the fault plane into subfaults and assumes each subfault to be a point source with a ω^{-2} spectrum. The length of the fault is taken as 85km and its width as 30km, and the fault plane is divided into 17×6 elements. Geometric spreading, regional anelastic attenuation and local site effect are included in the model. Satisfactory agreements between simulated and observed results validate capability of the method in prediction of ground motion in the study region

Keywords Stochastic model, Ground motion Simulation, Finite-Fault model, Tabas earthquake

چکیده هدف اصلی این مقاله، شبیه سازی حر کت های زمین در اثر زلزله 16 سپتامبر1978 طبس در شمال شرق ایران با استفاده از روش گسل های محدود می باشد . در این روش صفحه گسل به چند بخش کوچک (subfault) تقسیم شده و فرض می شود که هرکدام از این گسلها از مدل ω^{-2} تبعیت می کند. طول و عرض گسل در این مقاله به ترتیب 85 و 30 کیلومتر فرض شده و کل گسل به 17×6 المان تقسیم شده است. پس از اعمال پارامترهای موثر در مدل نظیر گسترش هندسی، کاهندگی غیر الاستیک مسیر و نیز اثرات ساختگاه، نتایج حاصل با رکورد های ثبت شده در ایستگاه های مختلف مقایسه شده است . همخوانی نسبتا خوب نتایج شبیه سازی ها ضمن تایید پارامترهای کالیبره شده برای این منطقه، توانایی مدل در پیش بینی های آینده را نیز نشان می دهد.

1. INTRODUCTION

Iran as one of the world's most earthquake-prone countries has been exposed to many destructive earthquakes in the past long years. The Iranian plateau is part of the major Eurasian plate with the tectonic setting of the region dominated by the collision of the Arabian, Eurasian and Indian plates in which the active deformation of Iran results from Arabia-Eurasia convergence. The Iranian plateau accommodates the 35mm/yr convergence rate between the Eurasian and Arabian plates by strike-slip and reverse faults with relatively low slip rates in a zone 1000km across [1]. During the twentieth century the Iranian people experienced at least one earthquake event exceeding magnitude 7 every seven years, and one event exceeding magnitude 6 every two years. These major events culminated in a very large death toll averaging 1,577 persons/year.

The large magnitude (mb = 6.4, Mw = 7.4) Tabas earthquake that occurred on September 16, 1978, in the east central Iran (Figure 1), is considered to be one of the most destructive regional events of the 20th century. The total death toll has been estimated to exceed 15,000 and the town of Tabas was seriously damaged [2, 3]. The earthquake was strongly felt over an area exceeding ~106km, with the highest intensity of shaking (IX-X MM) observed at the town of Tabas and the adjoining villages (see Figure 2 of Ref [3]) near the northern limit of the rupture. It was recorded by several accelerographs, and its peak acceleration varied between 0.95 and 0.01g in the

epicentral range from 3 to 350km. The town of Tabas was not identified as zone at high risk from seismic activity until this destructive earthquake occurred on fault near it.

The "stochastic modeling approach" has been extensively used in the past for the prediction of strong ground motion. Various earthquake source models such as the "ω^{-2} model" [4, 5] have been employed for this purpose [6]. A discrete finite-fault model that captures the salient features of radiation from large earthquakes has been a popular seismological tool over the past two decades. In this method, the fault plane is discretized into small independently rupturing subfaults and the radiation from all subfaults is summed at the observation point.

The essential ingredient for the stochastic method is the spectrum of the ground motion. This is where the physics of the earthquake process and wave propagation is contained, usually encapsulated and put into the form of simple equations (see Equation 1 in next section). It is a simple tool that combines a good deal of empiricism with a little seismology and yet has been as successful as more sophisticated methods in predicting ground-motion amplitudes over a broad range of magnitudes, distances, frequencies, and tectonic environments.

The objective of this study is to simulate ground motions from the 16 September 1978 Tabas, Iran, earthquake using of stochastic Finite fault modeling. Results of stochastic simulations correspond to calibrated parameters are validated against the observed in the selected stations.

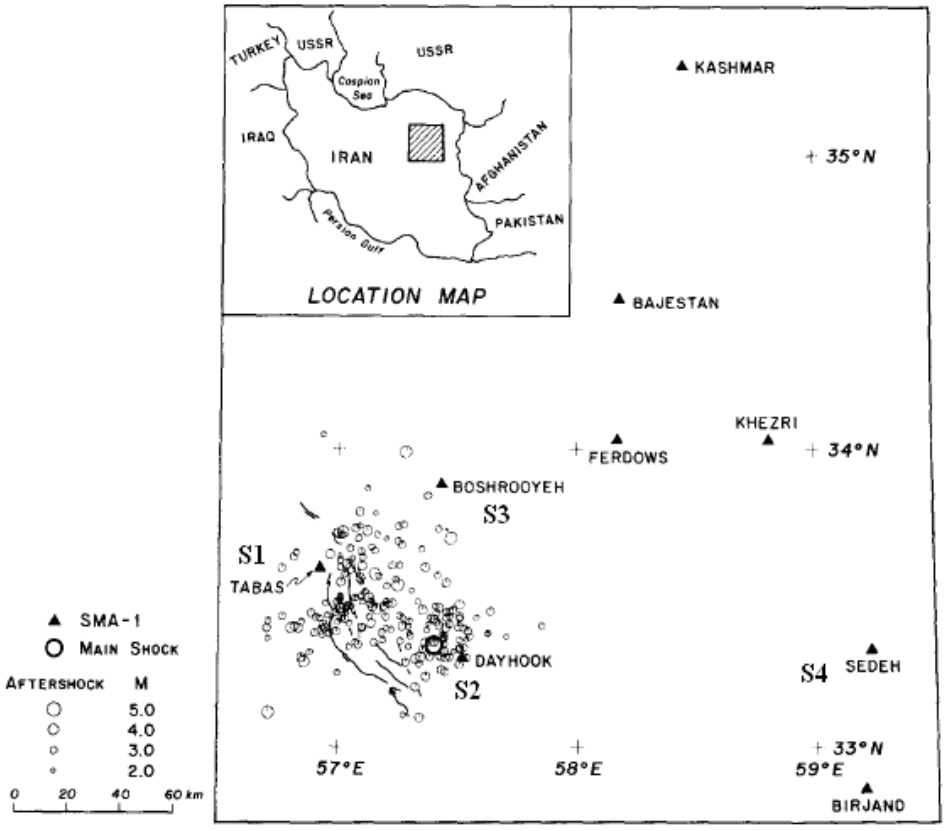

Figure 1 Map of the region adjacent to the Tabas, Iran earthquake [7]

2. STOCHASTIC SIMULATION METHOD

During the past decades, much attempt has been given in reliable simulation of strong ground motion that include theoretical or semi-empirical modeling of the parameters affecting the shape, the duration and the frequency content of strong motion records. The stochastic point source model stems out from the work of Hanks and McGuire [8] who indicated that the observed high frequency ground motion can be represented by windowed and filtered white noise, with the average spectral content determined by a simple description of the source. Many researchers have applied this method to simulate ground motion from point sources [9-12].

In this method, the horizontal component of desired acceleration amplitude spectrum $a(M,R,f)$, defined by a source and a propagation model, is a function of moment magnitude (M) and distance (R):

$$a(M,R,f) = C \times S(M,f) \times D(R,f) \times P(f) \times A(f) \quad (1)$$

Where C is a no constant given by $C = < R_{\varphi} > \times F \times V / 4\pi\rho\beta^3 R$ and $\langle R_{\upsilon\varphi} \rangle$ is the radiation pattern averaged over an appropriate range of azimuth and take-off angle, F accounts for free surface effects, V represents the partition of a vector into horizontal components. ρ, β are the crustal density and shear wave velocity respectively. *S(M,f)* is a source function, $D(R,f)$ is a seismic attenuation function filter, $P(f)$ is a high-frequency truncation filter and $A(f)$ is site amplification [11] .

The seismic attenuation function is represented by:

$$D(R,f) = G(R) \times e^{\frac{-\pi \times f \times R}{Q(f) \times \beta}} \quad (2)$$

where $G(R)$ is a geometric attenuation function caused by the changing of wave component along the distant, the second term is related to anelastic whole path attenuation and Q is the path-averaged frequency-dependent shear wave crustal quality factor, which is a regional dependent parameter and scattering within the deep crustal structure.

The $p(f)$ filter is the upper crust attenuation factor that is used to model the observation that an acceleration spectral density usually appears to fall off rapidly beyond a maximum frequency [13,14]. I applied high frequency filter $p(f)$ in the following form [15]:

$$p(f) = \exp(-\pi \times \kappa \times f) \quad (3)$$

The decay parameter Kappa (κ), represents the effect of an intrinsic attenuation upon the wavefield as it propagates through below the site. The simulation procedure is followed such that, the Fourier amplitude spectrum derived from the seismological model defines the frequency content of the earthquake ground motion. This frequency information is combined with a uniform random phase angles in a stochastic process to generate synthetic accelelograms.

3. STOCHASTIC FINITE-FAULT MODELING

Even though the success of the point-source model has been pointed out repeatedly, it is also well known that this model was developed on the basis of far-field and small earthquake record which is not exactly suitable for near-source strong ground motions [16,17]. So, further modifications in this model are required. Beresnev and Atkinson [16] have proposed a technique that overcomes the limitation posed by the hypothesis of a point source. Their technique is based on the original idea of Hartzell [18] to model large events by the summation of smaller ones. He used a summation technique consisting of a time delay to approximate the main event by using of records of foreshocks and aftershocks. This idea has been grown recently along with advance simulation methods such as stochastic finite fault method. In this approach, the fault plane is discretized into a finite number of subfaults, each of which is treated as a point source with a theoretical ω^{-2}, and radiations from all subsources are appropriately lagged in time and summed at the observation aimed site [16].

The corner frequency (f_0) and seismic moment (m_0) of the subfaults are derived in terms of

subfault size (Δl):

$$f_0 = {}^{(yz}\!/_{\pi)}\beta\,/_{\Delta l} \quad (4)$$

$$m_0 = \Delta\sigma\Delta l^3 \quad (5)$$

Where $\Delta\sigma$ is the Kanamori-Anderson [19] "stress parameter", fixed at 50 bar, β is the shear wave velocity, y is the fraction of rupture-propagation velocity to β (assumed equal to 0.8 in the present study), and z is a parameter physically linked to the maximum rate of slip. The value of z depends on the definition of the rise time and for standard conventions *z=1.68* [16,20]. Due to the uncertainties involved in the definition of *z*, its value is allowed to vary through a parameter called *sfact*, which practically consists a "free" parameter during the implementation of the method.
Finally, a randomized time-delay for each subfult radiation to reach the observation point is calculated and the generated time series is shifted and added to total wave field in time domain as:

$$a(t) = \sum_{i=1}^{nw}\sum_{j=1}^{nl} a_{ij}(t + \Delta t_{ij}) \quad (6)$$

Where nl and nw are the number of subfaults along the length and width of the main fault, respectively, Δt_{ij} is the time-delay from the radiated ij subfault wave. It should be noted that an element in fault plane triggers when rupture arrives its center. The contributions from all subfaults are lagged and then summed at the observation point. The time delay for a subfault is given by the time required for the rupture to reach the element, plus the time for shear wave propagation from the center of subfault to the receiver.

It is worth to note that, this method of ground motion modeling is known as a simple and authoritative method for simulating of ground motions which are more interesting for engineers, and it is extensively used to estimate ground motions for regions of the world that there are not sufficient recordings of motion from potentially damaging earthquakes [21,22,23].

4. MODELING PARAMETERS

Modeling of finite source requires information of the geometry of fault plane, as well as information of the dimensions of subfaults and the location of hypocenter. The trends of epicenteral and hypocenteral distribution are in accordance with the strike and dip angle of the focal mechanism (strike, dip, slip) = (332, 31,110) of the mainshock [3]. Based on analysis and co-seismic investigation of Berberian [3] over main shock, the source dimension is roughly estimated to be 85km x 30km and fault plane has been divided to 17×6 subfaults. The preferred length of fault can be verified by the empirical relationships of Wells and Coppersmith [24] that predict fault length (L) as a function of moment magnitude for earthquakes of all mechanisms; $Log\ L = -2.44 + 0.59M$, by applying the above equation, fault length is corresponding to 84.3km which is very close to proposed value in this study and reconfirms the assumption of paper for fault dimension. I adopted the location of the hypocenter at a depth of 9 km which determined using body wave inversion by Walker and et al., [25] and kept the value of stress drop to 50bar. There are several different, but associated, measures of the stress drop. From the perspective of geological observations, the static stress drop can be expressed in general and simple form called static stress drop which introduced by Kanamori and Anderson [19]. In stochastic finite fault modeling of ground motions, stress parameter is a parameter that controls each subfault moment and also the total moment summed over all subsources.

As recommended by Beresnev and Atkinson [16] to avoid an inadequate number of active subsources, the stress parameter is set to a value of 50 bars, the average static stress drop as introduced by Kanamori and Anderson [19]. The material properties represented by density ρ, and shear wave velocity β, were estimated to be 2.7 g/cm^3 and 3.5 km/s, respectively based on Global Crustal Model by Specification of 2×2 degree tiles surrounding around Tabas in CRUST 2.0 [26].

A geometric attenuation spreading operators $1/R$ for $R \le 70$ km, $1/R^0$ for $70 < R \le 130$ and $1/R^{0.5}$ for R>130km were applied. A mean frequency dependent quality factor $Q(f)$,

represented as the anelastic attenuation was used based on the relation proposed by Shoja-Taheri et al., [27] in the form of $Q = 350 f$.

According to previous studies Radiation-strength factor (*sfact*) that controls the strength of subfault radiation, usually takes the value of 1.5±0.3 [28, 29]. Although, theoretically it is between 0.5 and 2 (lower values correspond to unusually small slip velocities and vice versa). Physically, this will correspond to a change in maximum slip velocity on the fault proportionally to first power of *sfact*. In the all of our simulations, we assigned to *sfact* the average value of 1.6 which reproduces sufficient result as will be shown later on.

The site amplification factors employed in this paper are estimated using those proposed by Boore and Joyner [30] for various site characterized by the average shear-wave velocity over the upper 30m ($\bar{V}_{30}$). Nine stations recorded strong motions from Tabas earthquake. The accelerograms from the stations, Tabas, Deyhook, Boshrooyeh and Sedeh has been selected because the signal-to-noise ratio of these motions is large. The other motions recorded in this event are known as weak motion by peak ground acceleration lower than 0.01g and also with lower signal-to-noise ratio. Consequently, these motions could not be more imperative in earthquake engineering purpose and have not been selected in this paper.

The locations of the stations for which simulations are performed in this study are also shown in Figure 1 (S1-S4). The soil types of selected stations based on Iran 2800 Code [31], geographical coordinates and recorded PGA are presented in Table 1. It should be mentioned that, the average shear wave velocity of the stations to those of NEHRP Standard Code [32] classifications show that, the soil types A and B of NEHRP are equivalent to the soil type I and that of D is equivalent to soil type III of Iran Standard Code respectively.The effects of the near-surface attenuation were also taken into account by diminishing the simulated spectra by the factor $\exp(-\pi\kappa f)$. The decay kappa factor of the region is estimated by averaging over those from recorded accelerations correspond to 0.06 [7]. The modeling parameters used for the simulations are summarized in Table 2.

TABLE 1. Information of Selected Recorded Ground Motions

Stations	Coordinates		Soil Type	PGA(cm/sec)	
	Lat	Lon		L	T
Tabas (S1)	33.6	56.92	I	903	900
Deyhook (S2)	33.3	57.52	I	327	400
Boshroyeh (S3)	33.88	57.43	I	97	87
Sedeh (S4)	33.33	59.23	I	27	22

TABLE 2. Modeling Parameters

Parameters	Tabas earthquake
Fault Dimension(km)	85×30
Fault Orientation	Strike 332^0 ,dip 31^0
Mainshock moment magnitude(M)	7.4
Stress parameter(bar)	50
Subfault dimension(km)	17×6
Number of subfaults	102
Subfault corner frequency	0.49
Crustal shear wave velocity(km/sec)	3.5
Crustal density (g/cm^3)	2.7
Geometric spreading	$R \le 70$ km $\rightarrow$ 1/R $70 \prec R \le 130 \rightarrow 1/R^0$ $R \succ 130 km \rightarrow$ $1/R^{0.5}$
$Q(f)$	$350 f^1$
Windowing function	Saragoni-Hart
Kappa operator	0.06

5. RESULTS AND DISCUSSION

Acceleration time history recorded during the 1978 Tabas earthquake, has been simulated using the stochastic finite-fault method proposed by Beresnev and Atkinson [16,17,33] which has been applied widely for different tectonic [33-37] taking

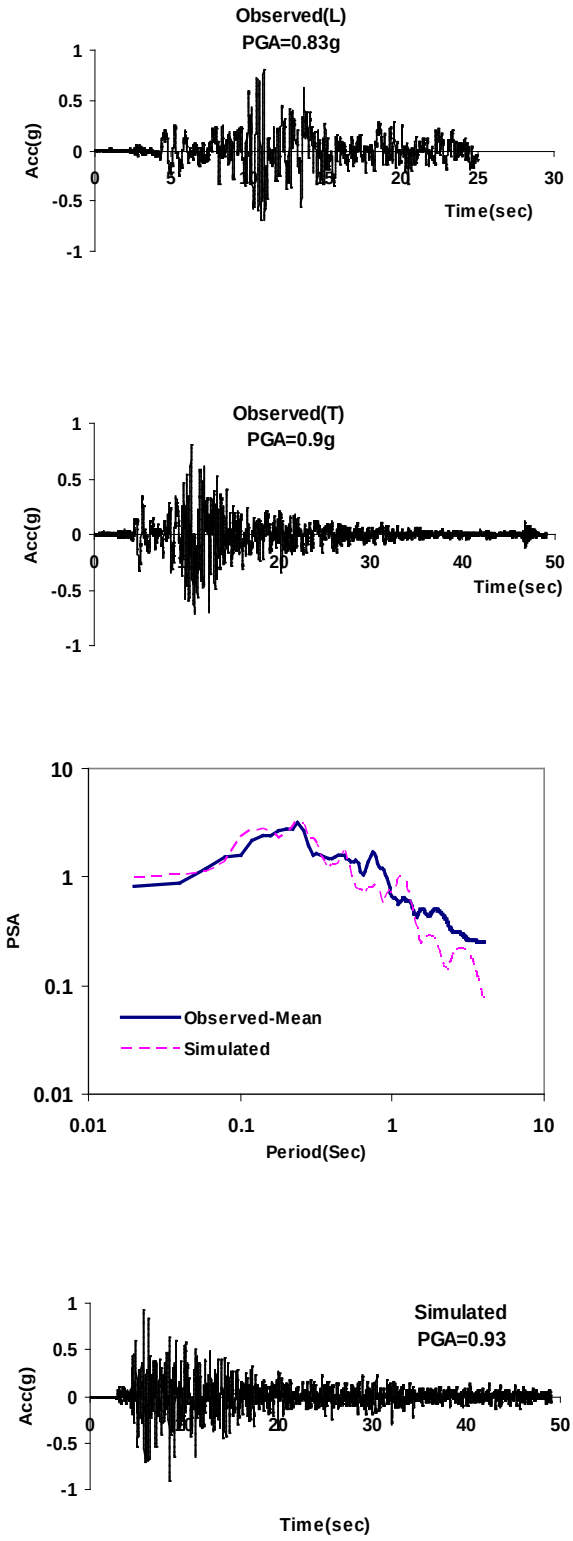

Figure 2 Simulated, observed pseudo-acceleration response spectra and acceleration time history at S1

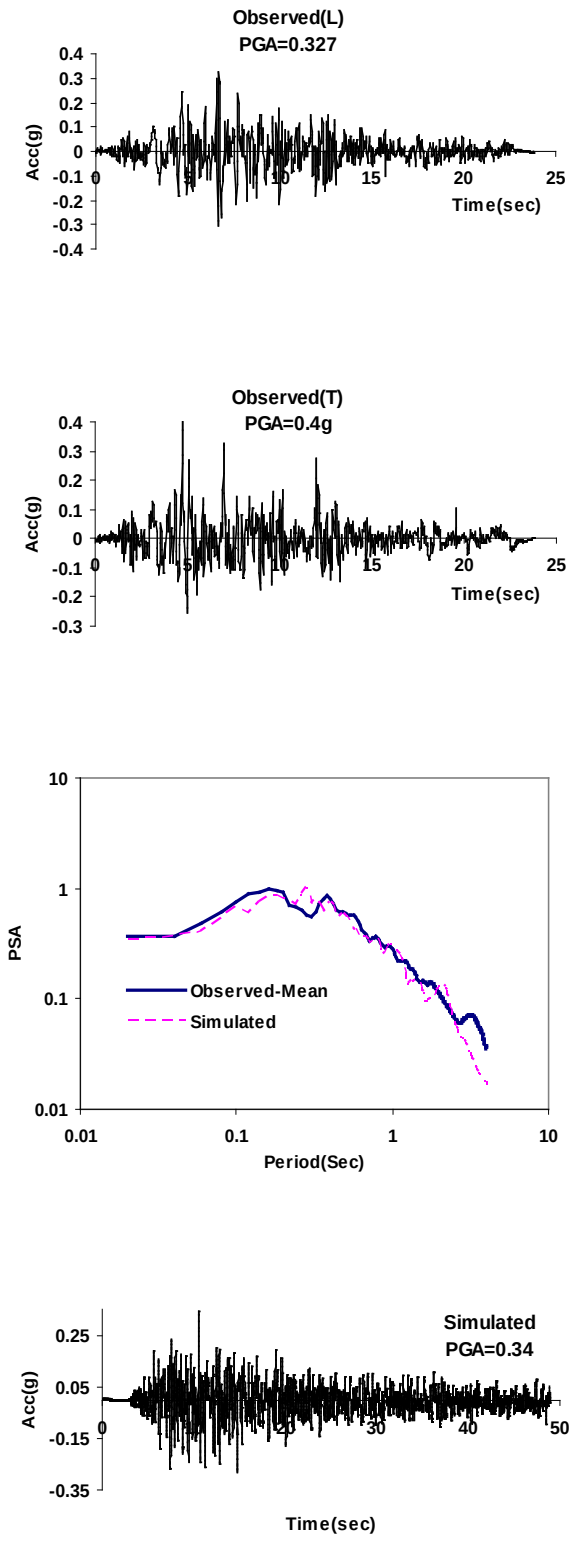

Figure 3 Simulated, observed pseudo-acceleration response spectra and acceleration time history at S2

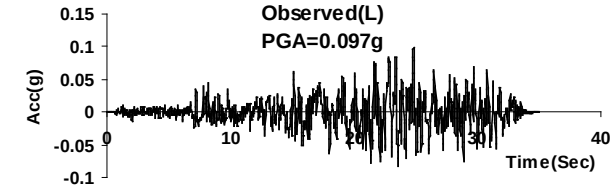

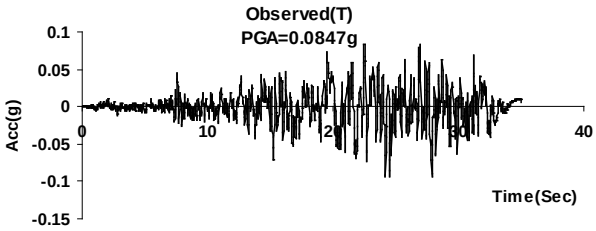

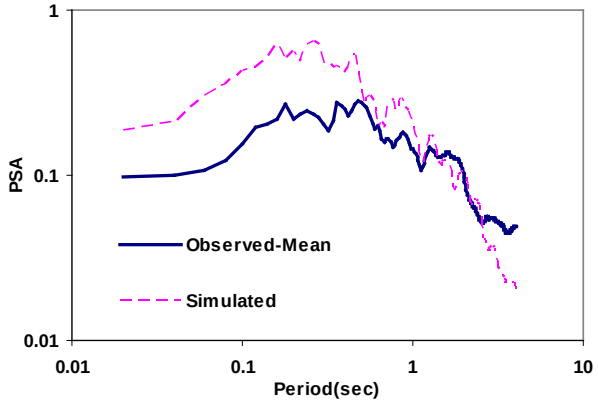

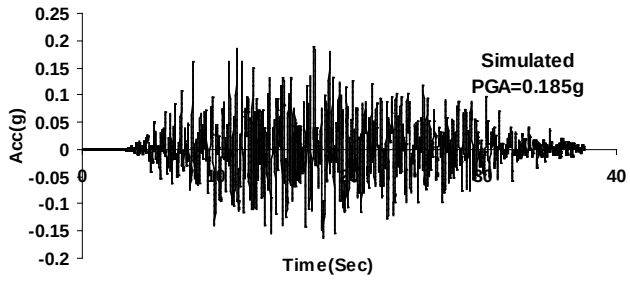

Figure 4 Simulated, observed pseudo-acceleration response spectra and acceleration time history at S3

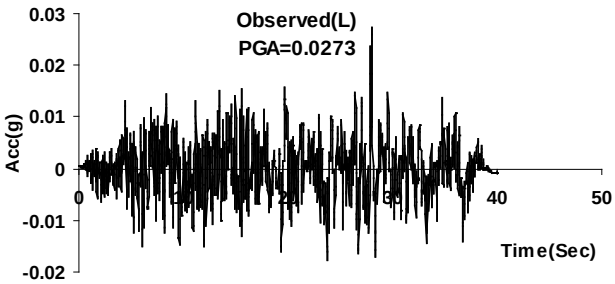

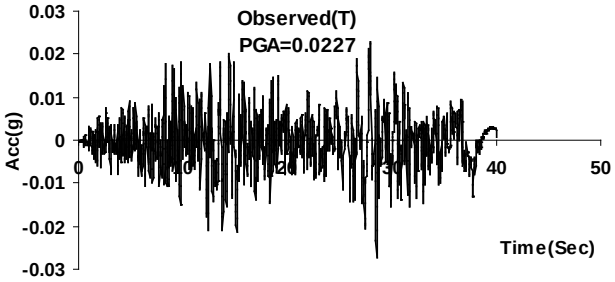

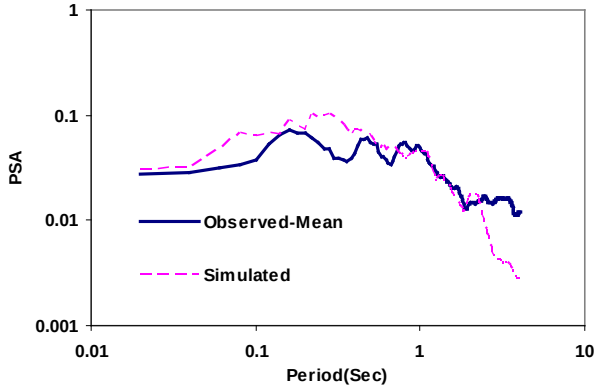

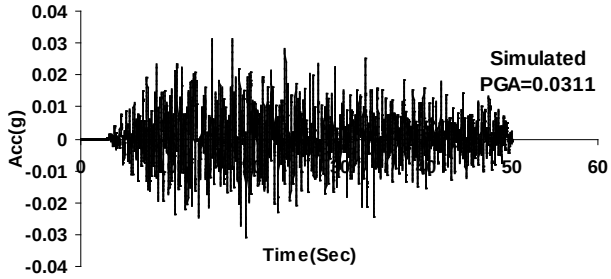

Figure 5 Simulated, observed pseudo-acceleration response spectra and acceleration time history at S4

The shape and amplitude of observed and simulated spectra show a good agreement within the intermediate- and high-frequency ranges at almost all stations. However, at low frequencies, the recorded amplitude spectra are generally larger than simulated. This can be viewed as the limitation of the homogeneous half space medium included in the simulation model to generate surface waves, which are generally observed on real accelerograms as well a Shoja-Taheri and Ghofrani [34] have concluded about 2003 Bam earthquake simulation with finite-fault modeling.

A significant discrepancy exists at Boshrooyeh station predominantly in high frequency (2-10 Hz) where the peak ground acceleration value is overestimated by almost a factor of 2. Because of well matched results at further stations, other effective parameters such as source model or path attenuation employed work successfully for them and this might be due to representation of the local site amplifications. Note, there is inadequate information over the near-surface (site) geology across different parts of Iran. Addressing this shortcoming, quantifying the site characteristics of every instrumented station in the network is more important and using of generic soil amplification will not leads to accurate results in all cases. So, Specific site effect corrections were required for the station in Boshrooyeh to achieve better match of the simulated results with lower amplifications factor. It is made in this paper by modifying of rock site condition to very hard rock sits. The revised results for Boshrooyeh station with better matching by recorded consequences shown in Figure 6. Peak ground acceleration and spectral shape and amplitude were considerably improved.

In this section also, a comparison between peak ground motions at Tabas, Dethook, Boshrooyeh and Sedeh with observed accelerograms could be produced. A notable agreement is obtain at all stations which corroborate the accuracy of proposed calibrated model for the study area.

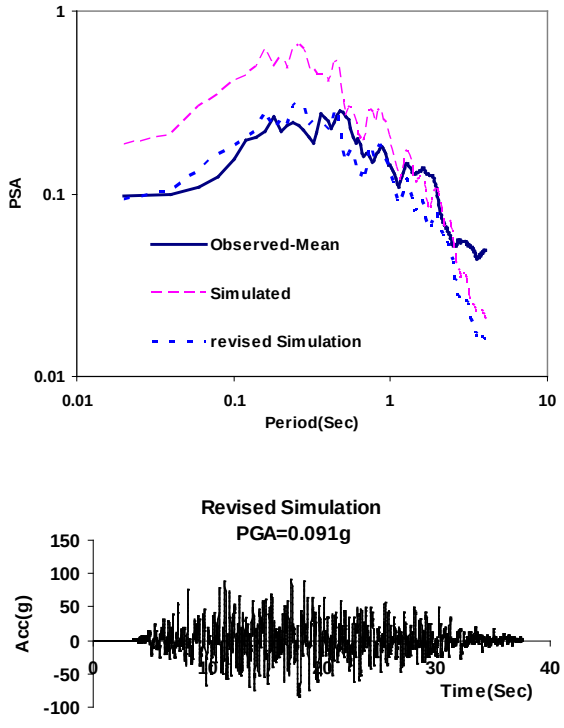

Figure 6 revised (simulation results) pseudo-acceleration response spectra and acceleration time history at S3

6. CONCLUSIONS

In this paper, the simulation wave with higher frequency components could be straightforwardly calculated by the stochastic finite fault technique, and this method was applied to synthesize the waves and to predict strong ground motions in the study area. Strong ground motions of 1978 Tabas earthquake in the east central Iran at four observation points were obtained, which are in good agreement with its recorded. The observed peak ground accelerations at all near and distant stations were significantly close to its simulated peak ground acceleration. Therefore, results obtained validate the accuracy of the determined parameters in proposed model for simulation of earthquakes in the study region.

The best match between the simulated and observed spectra is obtained when the hypocenter is set at the depth of 9km in the middle of the main fault with random distribution of slip. Since the random slip distribution used in the modeling allows correctly reproducing ground motions, the methodology applied in this study together with the calibration model that has been established form a very efficient tool for engineering applications. Consistent predictions of ground motion through analogous analysis, considering

similar geometry of the rupture and hypocenter locations, can be obtained for future events in the region for which the distribution of slip is not known.

It can be proposed to use the calibrated model for simulating historical or hypothetical earthquakes in the Tabas region for seismic hazard analysis or simulation of reliable ground motions purposes which the latest could be used for time history analysis of structures.

7. REFERENCES

1. Berberian, M. and R. S. Yeats "Patterns of Historical EarthquakeR upturei n the Iranian Plateau," ***Bull. Seism. Soc. Am***. Vol. 89, No. 1, (1999), 120-139.
2. Mohajer-Ashjai, A. and A. A. Nowroozi "The Tabas earthquake of September 16, 1978 in eastcentral Iran: a preliminary field report", ***Geophys. Res. Letters*** 6, (1979), 689-692.
3. Berberian, M. "Earthquake faulting and bedding thrust associated with the Tabas-e-Golshan (Iran) earthquake of September 16, 1978", ***Bull. Seism. Soc. Am.*** 69, (1979), 1861-1887.
4. Brune, J. N. "Tectonic stress and the spectra of seismic shear waves from earthquakes," ***J. Geophys. Res.*** 75, (1970), 4997–5009.
5. Frankel A, Mueller C, Barnhard T, Perkins D, Leyendecker EV, Dickman N, Hanson S, Hopper M. "National seismic-hazard maps. National seismic-hazard maps:" Documentation ***Open-File Report*** 96-532, (1996), U.S. Geological Survey, Reston, VA.
6. Atkinson, G. M. and D. M. Boore "Evaluation of models for earthquake source spectra in eastern North America," ***Bull. Seism. Soc. Am.*** 88, (1998), 917-934.
7. Shoja-Taheri J. and Anderson .J "The 1978 Tabas, Iran, earthquake: an interpretation of the strong motion records", ***Bull. Seism. Soc. Am,*** Vol. 78, No. 1, (1988), 142-171.
8. Hanks, T. C. and R. K. McGuire "The Character of High Frequency Strong Ground Motion," ***Bull. Seism. Soc. Am.*** 71, (1981), 2071–2095.
9. Boore, D. M. and G. M. Atkinson "Stochastic Prediction of Ground Motion and Spectral Response Parameters at Hard–Rock Sites in Eastern North America," ***Bull. Seism. Soc. Am***. 77, (1987), 440 – 467.
10. Toro, G. and R. McGuire "An Investigation into Earthquake Ground Motion Characteristics in Eastern North America," ***Bull. Seism. Soc. Am***. 77, (1987), 468–489.
11. Atkinson, G. M. and D. M. Boore "Ground – Motion Relations for Eastern North America," ***Bull. Seism. Soc. Am***. 85, (1995), 17 – 30.
12. Yazdani A. and Komachi Y. "Computation of Earthquake Response via Fourier Amplitude Spectra", ***International Journal of Engineering,*** Volume 22 - 2 - Transactions B: Applications, (2009), 147-152.
13. Hanks T.C. " $f_{\max}$," ***Bull. Seism. Soc. Am***. 72, (1982), 1867 – 1979.
14. Silva, W.J., and R. Darragh "Engineering characterization of earthquake strong motion recorded at rock sites," ***Palo Alto, Calif:*** Electric Power Research Institute, (1995), TR-102261.
15. Anderson, J. and S. Hough "A model for the Fourier amplitude spectrum of acceleration at high frequency," ***Bull. Seism. Soc. Am.*** 74, (1984), 1969-1993.
16. Beresnev, I. A. and G. M.Atkinson "Modeling Finite–Fault Radiation from the ωn Spectrum," ***Bull. Seism. Soc. Am. 87***, (1997), 67 – 84.
17. Beresnev, I. A. and G. M. Atkinson "FINSIM – a FORTRAN Program for Simulating Stochastic Acceleration Time Histories from Finite Faults," ***Seism. Res. Let.*** 69, (1998a), 27 – 32.
18. Hartzell, S. "Earthquake Aftershocks as Green's Functions," ***Geophys. Res. Let.*** 5, (1978), 1–4.
19. Kanamori, H. and Anderson, D. L. "Theoretical basis of some empirical relations in seismology," ***Bull. Seism. Soc. Am.*** 65(5), (1975), 1073-1095.
20. Beresnev, I. A. and G. M. Atkinson "Stochastic Finite-Fault Modeling of Ground Motion from 1994 Northridge Acceleration, California, earthquake. I-validation on Rock Sites," ***Bull. Seism. Soc. Am***. 88, (1998b), 1392 – 1401.
21. Castro1 R. R. and Ruíz-Cruz E. "Stochastic Modeling of the 30 September 1999 Mw 7.5 Earthquake, Oaxaca, Mexico", ***Bull. Seism. Soc. Am***, Vol. 95, No. 6, (2005), 2259-2271.
22. Ameri G., Gallovic F., Pacor F., and Emolo A., "Uncertainties in Strong Ground-Motion Prediction with Finite-Fault Synthetic Seismograms: An Application to the 1984 M 5.7 Gubbio, Central Italy, Earthquake", ***Bull. Seism. Soc. Am***, Vol. 99, No. 2A, (2009), 647-663.
23. Castro R. R., Pacor F., Franceschina G., Bindi D., Zonno G., and Luzi L. "Stochastic Strong-Motion Simulation of the Mw 6 Umbria–Marche Earthquake of September 1997: Comparison of Different Approaches", ***Bull. Seism. Soc. Am***, Vol. 98, No. 2, (2008), 662-670.
24. Wells, D.L. and Coppersmith K.J. "New empirical relationships among magnitude rupture length rupture width, and surface displacement", ***Bull. Seism. Soc. Am***, Vol. 84 (1994), 974-1002.
25. Walker J., J. Jackson and C. Baker "Surface expression of thrust faulting in eastern Iran: source parameters and surface deformation of the 1978 Tabas and 1968 Ferdows earthquake sequences", ***Geophys. J. Int***
26. Global Crustal Model CRUST2.0, Institute of Geophysics and Planetary Physics, University of California, San Diego, (2001), http://mahi.ucsd.edu/Gabi/rem.dir/crust/crust2.html.
27. Shoja-Taheri, J.,Naseri,S. and Ghafoorian, A. "The 2003 Bam, Iran, Earthquake :An interpretation of strong motion records," ***Earthquake Spectra***,Vol.21,No.S1,

(2005), 181-206.
28. Beresnev, I. and Atkinson, G "Subevent structure of large earthquakes – A ground motion perspective," ***Geophys. Res. Lett.*** 28, (2001a), 53–56.
29. Beresnev, I. and Atkinson, G "Correction to Subevent structure of large earthquakes – A ground motion perspective," ***Geophys. Res. Lett.*** 28, (2001b), 46–63.
30. Boore, D. M. and W. B. Joyner "Site Amplification for Generic Rock Sites", ***Bull. Seism. Soc. Am***. 87, (1997), 327 – 341.
31. Iranian Code of Practice for Seismic Resistant Design of Building (Standard No: 2800), Third Edition 2006, Building and Housing Research Center (BHRC), (in Persian).
32. NEHRP Recommended Provisions and Commentary for Seismic Regulations for New Buildings and Other Structures, 2003 Edition.
33. Beresnev, I. A. and G. M.Atkinson "Source Parameters of Earthquakes in Eastern and Western North America Based on Finite-Fault Modeling," ***Bull. Seism. Soc. Am***. 92, (2002), 695 – 710.
34. Shoja-Taheri J. and Ghofrani H. "Stochastic finite-fault modeling of strong ground motions from the 26 December 2003 Bam, Iran, earthquake", ***Bull. Seism. Soc. Am,*** Vol. 97, No. 6, (2007), 1950–1959.
35. Roumelioti Z. and Kiratzi A. "Stochastic Simulation of Strong-Motion Records from the 15 April 1979 (M 7.1) Montenegro Earthquake", ***Bull. Seism. Soc. Am,*** Vol. 92, No.95, (2002), 1095-1101.
36. Christoforos A. Benetatos and Kiratzi A. "stochastic strong ground motion simulation of intermediate depth earthquakes: the cases of the 30 May 1990 Vrancea (Romania) and of the 22 January 2002 Karpathos island (Greece) earthquakes", ***Soil Dynamics and Earthquake Engineering,*** Vol .24, Issue 1, (2004), 1-9.
37. Roumelioti Z., Kiratzi A. and Theodulidis N. "Stochastic Strong Ground-Motion Simulation of the 7 September 1999 Athens (Greece) Earthquake", ***Bull. Seism. Soc. Am***, Vol. 94, No. 3, (2004), 1036-1052.
38. Yaghmaei-Sabegh S. and Lam N.TK "Ground motion modelling in Tehran based on the stochastic method" ***Soil Dynamics and Earthquake Engineering,*** Vol 30, (2010), 525-535.